CHARACTERIZING EPITHELIAL-MESENCHYMAL-TRANSITION (EMT)-LIKE BEHAVIOR IN BREAST CANCER CELLS IN A TISSUE ENGINEERING CO-CULTURE MODEL

An Undergraduate Research Scholars Thesis

by

AMANDA RAKOSKI

Submitted to the Undergraduate Research Scholars program at
Texas A&M University
in partial fulfillment of the requirements for the designation as an

UNDERGRADUATE RESEARCH SCHOLAR

Approved by Research Advisor: Dr. Daniel Alge

May 2020

Major: Biomedical Engineering

TABLE OF CONTENTS

ABSTRACT

Characterizing Epithelial-Mesenchymal-Transition (EMT)-Like Behavior in Breast Cancer Cells in a Tissue Engineering Co-Culture Model

Amanda Rakoski
Department of Biomedical Engineering
Texas A&M University

Research Advisor: Dr. Daniel Alge
Department of Biomedical Engineering, Department of Materials Science
Texas A&M University

Tissue engineered 3D cell culture models have shown promise investigating the influence of the tumor microenvironment on cancer cell behavior. Synthetic hydrogels, such as those made from poly(ethylene glycol) (PEG), can be customized with bio-instructive moieties that mimic different parts of the extracellular matrix (ECM) that cells can adhere to through integrins and regions of cadherins that cells can interact with through their own cadherins. The question remains of how the composition of the ECM and neighboring cell interactions impact the transition from an epithelial phenotype to a mesenchymal-like phenotype, termed EMT, which is considered crucial in tumor progression to metastatic cancer. Therefore, in this project, a cell-adhesive peptide that mimics ECM and an cadherin mimetic peptide that mimics mesenchymal N-cadherin were utilized to investigate how cell-ECM interactions through integrin binding and how cell-cell interactions through cadherin binding can direct the emergence of EMT markers in breast cancer. Cytotoxicity studies demonstrated that the peptides allowed high SKBR3 breast cancer cell cytocompatibility but significantly lowered 3T3 fibroblast viability in a 3D environment, indicating that the peptide interactions were changing the behavior of the 3T3's in

a way that did not affect the SKBR3's. Also, encapsulated as single cells in a gel with a cell-ECM peptide, the 3T3's began to obtain a spindle-like phenotype, but not the SKBR3's, showing that the 3T3's were starting to form focal adhesions and take on a more mesenchymal-like phenotype not taken on by SKBR3's in the same conditions. When putting the 3T3's and SKBR3's in co-culture, the SKBR3's obtained a spindle-like phenotype when the 3T3's were in a gel with a cadherin peptide, showing the beginning of an epithelial-mesenchymal transition-like morphology. After running quantitative PCR on said SKBR3's, it was found that SKBR3's with 3T3's in contact with both cell adhesive and cadherin peptide and without either peptides were making significantly more mRNA for Collagen III and vimentin than SKBR3's in contact with 3T3's in only a cell-ECM peptide gel, both proteins made as a sign of becoming more mesenchymal-like. Collectively, these results demonstrate that the ability to incorporate mimetic peptides of cell-cell and cell-ECM interaction into PEG hydrogels makes them a powerful platform for studying how the composition of the ECM impacts EMT.

ACKNOWLEDGMENTS

I would like to give a huge thanks my principal investigator, Dr. Alge, as he took a chance on me 3.5 years ago when he let me join his lab as a freshman and has supported me in all my research endeavors ever since. I am so grateful he has given me so many opportunities to learn and grow and has believed in my abilities even sometimes more than I believe in myself. Also, I would like to thank my graduate student teacher, Samantha Holt, as she has taught me about cancer and experiments since the beginning of my time in the Alge lab, taking on the challenge of teaching their first undergraduate student in her first months of graduate school. We have both grown together during our time, and I am thankful for her helping see where my passions lie.

Thanks also go to my friends and colleagues and the department faculty and staff for making my time at Texas A&M University an experience that has shown me a future career option I would have never seen without their support. Also, thanks to the Women in Engineering program who have provided me the opportunity to do research in my undergraduate years with the Clare Boothe Luce Scholarship. Special thanks to the Kaunas lab for always being there to help me with the equipment for RNA work and thank you to the Gaharwar lab for always being there for conversation through my most tough times as when I spent many evenings and long weekends working alone, they would be there, keeping me company and checking on my wellbeing. Thank you to Michael R Raulerson from the TAMU chemistry department who has always had a smiling face as he ran all my many peptide samples through MALDI+ and ESI+.

Finally, thanks to my mother and father for their support as I have gone through these many years of research.

NOMENCLATURE

ECM	Extracellular Matrix
PEG	Poly(ethylene glycol)
RGD	Peptide that mimics extracellular matrix for integrin-mediated cell adhesion
HAVDI	Peptide that mimics N-cadherin and used in cell-cell interaction
RDG	Peptide scramble that does not allow cell adhesion
KCGPQ-W	Degradable peptide crosslinker

CHAPTER I

INTRODUCTION

In the human body, cell behavior is directed by interacting with other cells through transmembrane receptors called cadherins and by interacting with the extracellular matrix (ECM), or the 3D network of polysaccharides and proteins surrounding cells, through transmembrane receptors called integrins. Cadherins are a family of transmembrane glycoproteins that are dependent on calcium to promote homotypic cell–cell adhesion and modulate tissue architecture as well as motility. Integrins are calcium independent cell adhesive molecules which promote heterotypic binding to proteins within the ECM such as including laminin, fibronectin, collagens, and more molecules (Bellis).

Cancer cells have been found to have E-cadherin and N-cadherin and their expression on the surface has been found to change as to transition from an epithelial-like phenotype to a mesenchymal-like phenotype, termed EMT. Increased N-cadherin expression and decreased expression of E-cadherin has been found to increase invasion and motility and therefore is considered to be associated with mesenchymal-like behavior preparing for metastasis (Nieman et al.). Also, as cancer cells become less epithelial-like and more mesenchymal-like, they are more inclined lose their sheet-like organization seen in epithelial cells by E-cadherin interaction as well as interaction with the basement membrane ECM and focus energy on remodeling ECM to promote tumorigenesis and to adhere to ECM in preparation for metastasis (Hamley; Pradhan et al.; Koistinen and Heino). Other characteristics of EMT are loss of apical-basal polarity, resistance to apoptosis, cytoskeleton reorganization, spindle-like phenotype more seen in mesenchymal cells, increased proliferation, bypassing of cell cycle signals to stop mitosis, and

downregulation of epithelial proteins (Lamouille, Xu and Derynck; Hanahan and Weinberg; Pickup, Mouw and Weaver). Cancer cells will even recruit and reprogram surrounding cells such as fibroblasts, macrophages, and immune cells similar to those involved in wound healing in order to shield itself from any anti-tumorigenic attacks (Foster et al.).

Tissue engineered 3D cell culture models have shown promise for investigating the influence of the tumor microenvironment on cancer cell behavior by simulating the mechanical and biomechanical properties found in human tissue (Holt et al.). Synthetic hydrogels are of current interest in mimicking the tumor microenvironment in vitro since the complexities of the tumor microenvironment can be difficult to isolate in vivo and in natural materials where an abundance of natural cell adhesive sites are available for cell interactions. Poly(ethylene glycol) (PEG) hydrogels are emerging to be an innovative material used for disease models since the PEG polymer is a bioinert, "blank slate" material which does not chemically interact with proteins or cells and allows for the tunability of the gel's mechanical and chemical properties. Also, since the cells cannot bind to the PEG polymer, the incorporation of user-defined binding sites such as ECM and cadherin mimetic peptides by "click chemistry" makes PEG-peptide gels a powerful platform for studying how the composition of the ECM and cadherins available for cell interaction impact cancer EMT (Lim et al.; Wu, Grande-Allen and West; Pradhan et al.; Yang et al.). Therefore, we utilized peptides with amino acid sequence Arginine-Glycine-Aspartic Acid (RGD), a cell-adhesive motif, and an amino acid sequence Histidine-Alanine-Valine-Aspartic Acid-Isoleucine (HAVDI), a N-cadherin motif, alone and in combination in poly(ethylene glycol) (PEG) hydrogels to encapsulate fibroblasts and breast cancer cells in order to look at changes in cell behavior such as in viability, phenotype, mRNA production contributed

to cell interactions with the synthetic mimetic peptides. Cell-cell interactions and cell-ECM interactions mimicked by peptides HAVDI and RGD are featured in **Figure 1**.

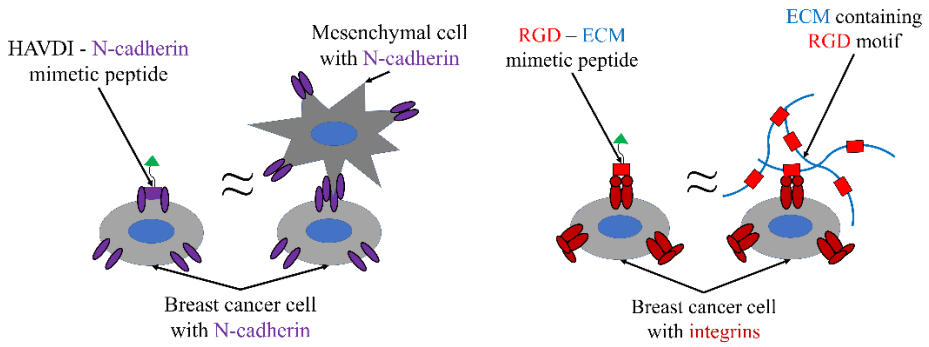

Figure 1. Cell interactions with cell signaling peptides

The cell-adhesive peptide we chose was with the motif RGD since RGD is a ubiquitous amino acid sequence commonly found on many ECM proteins such as collage, fibronectin, vitronectin, and laminin, has affinities to multiple integrin receptors, and has been utilized in multiple synthetic models of tissue to direct cell behavior (Nieberler et al.; Gu and Masters; Bellis). RGD has also been utilized in models of cancerous tissue in order to understand integrins' role in the development of cancer as well as the changes in integrin expression and the development of focal adhesions in cancer in the context of cell migration, spheroid formation, angiogenesis, and EMT (Weiss et al.; Fischbach et al.; Pradhan et al.; Singh et al.; Wang et al.). In nature, integrins on cells have two subunits (alpha and beta) which pair together to bind to ECM proteins. Pairings of different regions on the subunits dictate ligand specificity such as the subunit pairing alpha5beta1 bind to fibronectin. Since RGD is found on multiple types of ECM proteins, it is a useful amino acid sequence to synthesize that integrins recognize and bind to (Koistinen and Heino; Nieberler et al.; Yamada).

The cadherin peptide we chose was with the motif HAV since HAV is found on N-cadherin and supports cell-cell adhesion between mesenchymal cells such as mesenchymal stem cells, neurons, and fibroblasts. An N-cadherin contains five extracellular ectodomains which link to f-actin intracellularly in order to prepare the cell for membrane protrusion by actin reorganization. The cell-cell interaction is formed by heterotypic (or cis) and homotypic (or trans) adhesion by N-cadherins. In trans-adhesion, meaning between N-cadherins on two different cells, one cell's tryptophan residue (W) docks into another cell's hydrophobic pocket on the first ecto-domain containing an alanine residue (A). While the tryptophan is docking into the hydrophobic pocket, both tryptophan residues' sidechains interact, strengthening the trans-adhesion. In cis-adhesion, meaning between N-cadherins on the same cell, the histidine (H) and valine (V) residues on the first ectodomain on one N-cadherin interact with a recognition sequence on a second ectodomain on a different N-cadherin on the same cell, strengthening the opposite N-cadherin adhesion with accumulating more N-cadherins from the same cell (Mrozik et al.; Blaschuk). By synthesizing the HAV motif already found in the first ectodomain of N-cadherin, the peptide can interact in both forms of cell-cell adhesion facilitated by N-cadherins. The addition of aspartic acid (D) and isoleucine (I) to the HAV motif forms HAVDI which specializes the peptide to recognized to only N-cadherin instead of other cadherins such as E-cadherin (Lim et al.). The mechanism of N-cadherin interactions proposed are supported with computational modelling in silico (Perez and Nelson; Harrison et al.). The cell-cell interaction by cells and mimicked by the HAVDI peptide can be seen in **Figure 2**.

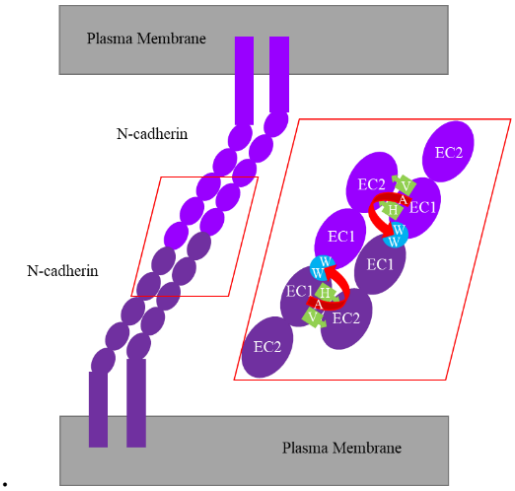

(A)

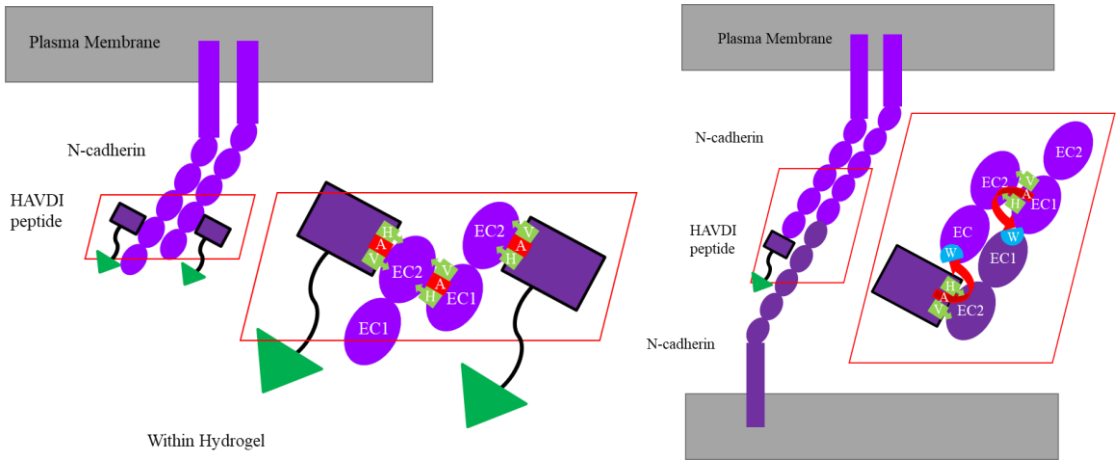

(B)

Figure 2. N-cadherin interactions **(A)** between two cells and **(B)** between a cell and the HAVDI peptide

The HAVDI peptide has recently been used to synthetically change cell behavior of mesenchymal cells and neuronal cells which express N-cadherin in nature (Williams, Williams and Doherty; Bian et al.; Cosgrove et al.). Interestingly, utilizing the HAVDI peptide in synthetic material has shown various effects on cell behavior. Generally, researchers have assumed that the monomeric versions of HAVDI are antagonists of cellular N-cadherin as the synthetic

HAVDI would compete against natural HAV in N-cadherins for attachment seen when linear HAVDI inhibited cadherin-dependent biological processes in neurons (Williams et al.; Blaschuk). In contrast, there have been studies where a linear HAVDI peptide served as an agonist of cellular N-cadherin as attachment of cells to HAVDI supported cell survival in stressful environment and cell differentiation in embryonic stem cells and mesenchymal stem cells (Lim et al.; Bian et al.). Despite the controversy over how the interaction between the HAVDI peptide and the HAV motif on the cell changes cell behavior, all these studies have shown that the HAVDI peptide can be used as a synthetic model of N-cadherin.

Murine 3T3 fibroblasts and human SKBR3 breast cancer cells can be utilized by themselves and in a co-culture since cancer has been seen to recruit fibroblasts to model the tumor microenvironment. Also, since fibroblasts have N-cadherin, they would directly interact with the HAVDI peptide. In contrast, the SKBR3's have no cadherins in normal culture conditions so how the cells interact with the HAVDI peptide is open for research (Hazan et al.). A fibroblast is a mesenchymal cell that is in the stroma to produce collagen and other ECM for the interstitial matrix and remodels the ECM by adhering to the ECM and releasing proteases called matrix metalloproteinases (MMPs) which ultimately changes ECM stiffness and available adhesion sites of the proteins. Cancer cells activate available transforming growth factor beta (TGF-β), platelet-derived growth factor, in the ECM or secreted by malignant cells in order to attract fibroblasts and transform normal fibroblasts to cancer-associated fibroblasts (CAFs) within the tumor tissue. Then CAFs work to create a tumor niche where collagen is turned from a dysregulated mass to aligned, crosslinked fibers in a process called desmoplasia and increase expression of myofibroblast markers such as alpha-smooth muscle actin (α-SMA), vimentin, and fibronectin.

With fibroblasts in co-culture with non-malignant cancer cells, it has been found to increase cancer cell survival and proliferation as well as cause the cancer cell phenotype to become more mesenchymal-like in vitro (Zeltz et al.; Koh et al.; Wei et al.; Wen et al.).

Therefore, the objective of this project was to characterize EMT-like behavior in breast cancer cells when in co-culture model with fibroblasts encapsulated in a PEG hydrogel with RGD and HAVDI peptides.

CHAPTER II

EXPERIMENTAL

Materials

8-arm, 40 kDa PEG-hydroxyl (PEG-OH) was purchased from Laysan Bio. Rink amide MBHA resin (100–200 mesh) was purchased from Novabiochem. Fmoc protected amino acids, 2-(1H-benzotriazol-1-yl)-1,1,3,3-tetramethyluronium hexafluorophosphate (HBTU), and N-methyl-pyrrolidinone (NMP) were purchased from Chem-Impex International Inc. 4-(Dimethylamino)pyridine (DMAP), anhydrous pyridine (biotech grade >99.9% grade), diisopropyl ethylamine (DIEA), deuterium oxide (D2O), phenol, piperidine – rea-gentplus (99%), triisopropylsilane (TIS), tri-fluoroacetic acid (TFA) reagent grade and HPLC grade, and sterile phosphate-buffered saline (PBS) were purchased from Sigma Aldrich. N,N'-Diisopropylcarbodiimide (DIC) and anhydrous piperazine (99%) were purchased from Alfa Aesar. 5-norbornene-2-carboxylic acid (98%), anhydrous diethyl ether, dichloro-methane (DCM)/methylene chloride, HPLC grade water and acetonitrile, 0.4% trypan blue solution, and McCoy's 5A Me-dium were purchased from Thermo Fisher Scientific. Dulbecco's Modified Eagle Medium (DMEM) was purchased from Corning. HOBt Hydrate was purchased from CreoSalus. Dulbecco's Modified Eagle Medium (DMEM) and 25% Trypsin 10X were purchased from Corning. Fetal bovine serum (FBS) was purchased from Atlanta Biologicals. 100X Penicillin streptomysin (Pen Strep) was purchased from EMD Millipore. Calcein-AM was purchased by MarkerGene Technologies Inc. Ethidium homodimer-1 was purchased from Chemodex. DAPI (hydrochloride) was purchased from Biolegend. Rhodamine phallodin was purchased from Biotium.

Synthetic procedures

Functionalization of PEG

8-arm, 40 kDa PEG-hydroxyl were functionalized with norbornene acid to produce octa-functional PEG-norbornene (PEG-NB), and functionalization was validated via NMR spectroscopy as previously described (Jivan et al.) to yield octa-functional PEG-norbornene (PEG-NB). All scales are relative to hydroxyls on PEG. To start anhydrous DCM, DIC (5x to PEG-OH), and norbornene acid (10x to PEG-OH) were added to a reaction vessel and allowed to react and mix under argon gas for 45 minutes at room temperature to generate a di-norbornene anhydride. Meanwhile, in a separate round bottom flask, 8-arm PEG macromer and DMAP (0.5x to PEG-OH) were dissolved in anhydrous DCM until completely dissolved (~ 5 min). Then pyridine was added to the round bottom flask containing PEG and allowed to stir for 15 minutes under argon gas. Finally, contents of the reaction vessel were filtered to remove precipitated urea salts and then added to the round-bottom flask containing PEG. The solution was allowed to react overnight at room temperature, and then was precipitated in 10-fold vol. excess of diethyl ether chilled to -20°C. The solution was vacuum filtered with a Buchner filter to yield a white precipitate of functionalized PEG. The product was then filtered twice and dried under vacuum for 24 h, dialyzed against deionized water for 2 days (MWCO = 10 kDa), and lyophilized to obtain purified 8-arm PEG-norbornene (structure in **Appendix**). Analysis of PEG-NB in D2O by 1H NMR indicated quantitative 87.5% end group functionalization with norbornene for octa-functional PEG. 1H NMR (500MHz, CDCl3) δ 6.19 – 5.90 (alkene protons from norbornene, m, 2H per end group), 4.26 – 4.12 (ester protons, m, 2H per end group), 3.73 – 3.54 (ethylene glycol protons, m, ~454H per arm of PEG-NB, ~181H for NB-PEG-NB).

Synthesis of peptide sequences

Peptide synthesis was performed on Rink amide resin with a microwave assisted peptide synthesizer (CEM DiscoverBio) using standard Fmoc solid phase peptide synthesis and HBTU activation with 0.5 mM DIEA in NMP (Chan and White). Resin was swelled in NMP and stirred with nitrogen gas bubbles for 30 minutes before all further reactions. Fmoc protecting groups were deprotected with 20% w/v piperidine in NMP for 5 min at 75°C except for aspartic acid (D) where 5% w/v piperazine with 0.1 M HOBt in NMP was utilized in order to prevent aspartamide formation. Deprotected amino acids were coupled for 8 minutes at 75°C, except for cysteine (C) and arginine (R) which were performed for 6 min at 50°C, and 25 min at room temperature then 5 min at 75°C, respectively. Capping of un-reacted amine groups were performed with 10% acetic anhydride in NMP for 2 minutes at 55°C. After the amino acids were all coupled, capped, and washed, the peptide was cleaved from resin by washing with DCM, then treating with 90 : 5 : 2.5 : 2.5 (TFA : phenol : TIS : water) cleavage solution for 2 h at room temperature followed by precipitation in cold diethyl ether. The peptide in diethyl ether was centrifuged, decanted, and dried completely under vacuum before purification. Crude peptide was purified by reverse-phase high performance liquid chromatography (HPLC, Thermo Scientific UltiMate 3000 with Agilent Technologies C18 column) with acetonitrile with 0.1% TFA and water with 0.01% TFA. After collecting the purified peptide in water, the purified product was analyzed via matrix assisted laser desorption ionization time of-flight mass spectrometry (MALDI-TOF MS) for peptides of greater than 1000 g/mol and electrospray ionization mass spectroscopy (ESI-MS) to verify peptide composition by molecular weight. Lyophilized pure peptides were dissolved in PBS and absorbance measurements at 205 nm and 280 nm (BioTek Synergy HT) were taken to calculate the stock concentrations (Anthis and Clore). KCGPQGIWGQCK (KCGPQ-W) was our matrix-

metalloproteinase (MMP) enzymatically degradable peptide, bi-functional from the thiol-containing cysteines (C) (Patterson and Hubbell). HAVDIGGGC (HAVDI) was the N-cadherin mimetic peptide found on the first ecto-domain on N-cadherin that strengthens the homotypic bonding between N-cadherins, monofunctional from the thiol-containing cysteine (C). CGRGDS (RGD) was the ECM mimetic peptide that had the RGD motif found on a bulk of ECM components such as fibronectin and laminin that cells can adhere to through integrin binding, monofunctional from the thiol-containing cysteine (C). CGRDGS (RDG) was the peptide scramble that had the RGD scrambled in order to inhibit cell adhesion, monofunctional from the thiol-containing cysteine (C) (all structures in **Appendix**). KCGPQ-W and RGD were verified by MALDI-TOF MS and monofunctional peptides HAVDI and RDG were verified by ESI MS because they were less than 1000 g/mol. MALDI-TOF MS: KCGPQGIWGQCK [M + H] = 1305 (expected), 1303.463 (found); CGRGDS [M + H] = 1188.513 (expected), 593.457 (found). ESI MS: HAVDIGGGC [M + H] = 827.359 (expected), 827.381 (found); CGRDGS [M + H] = 593.222 (expected), 593.245 (found); CGRGDS [M + H] = 593.222 (expected), 593.245 (found). All MALDI+ and ESI+ graphs are in **Appendix**.

Methods

Synthesis of hydrogels

Stock solutions were prepared by suspending polymer and peptide powder in PBS to desired concentrations: 20 wt% 8-arm, 40 kDa PEG-NB, 100 mM KCGPQ-W, 50 mM HAVDI, 50 mM RGD, 50 mM RDG. PEG hydrogel precursor solutions were crosslinked via thiol–ene click chemistry. Briefly, 5 wt% 8-arm PEG-NB was combined with a KCGPQ-W crosslinker ([thiol] : [norbornene] ratio of 1 : 2), 1 mM of one monofunctional cell adhesive peptide, 1 mM of second monofunctional cell adhesive peptide, and lithium acylphosphinate photoinitiator (LAP, 2 mM), synthesized as previously described (Fairbanks et al.). Various combinations of peptides were chosen for experimental groups. 3T3 fibroblasts or SKBR3 breast cancer cells were resuspended in order to achieve 20,000 cells/20 ul gel and added to the precursor solution in all cell studies. Cell media was added to gain a volume of 20 ul per gel for cell studies. Precursor solution was added to 6 mm syringe-tip molds and photopolymerization was achieved using UV light (Omnicure S2000 with a 365 nm filter) at 5 mW/cm2 for 3 minutes (**Figure 3**).

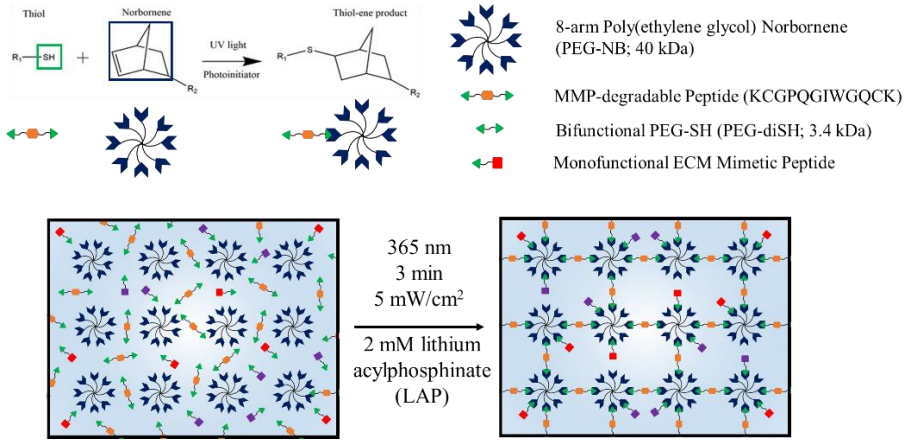

Figure 3. Hydrogel formation

For mechanical characterization, gels were made without cells and having PBS replace the volume of cell media to achieve 60 ul. The precursor solution was added to 1 mm thick, 8 mm diameter gasket molds on top of Sigmacoted glass slides and then photopolymerized with UV light at 5 mW/cm^2 for 5 minutes.

Rheology

To measure storage modulus of the hydrogels, 60 ul hydrogels were made without cells as previously described and swelled in ultrapure water for 24 hours. Then the hydrogels were cut with an 8 mm diameter biopsy punch in order to fit the 8 mm circular rheology tool. Finally, the storage modulus was measured by applying a normal force 0.03 N continuously on the gel and running a time sweep with frequency of 1 rad/s and 1% strain for 60 seconds at 37°C on an Anton Parr rheometer.

Swelling Ratio

To measure the swelling ratio of the hydrogels, hydrogels utilized for rheology were weighed wet with a balance, dried in a desiccator for 24 hours, and then weighed again dry. The calculation used for swelling ratio was Q = (Ws-Wd)/Wd where Ws is mass of swollen gel and Wd is mass of dry gel.

3T3 Fibroblasts Culture and SKBR3 culture

NIH 3T3 fibroblasts were purchased from ATCC and expanded in DMEM with 10% FBS and 1X Pen/Strep on polystyrene culture plates at 37 °C and 5% CO2 in a humidified environment until 70% confluence, ending culture at passage number 30. In passaging, the media was aspirated, cells were washed with PBS, trypsinized with 1X Trypsin, incubated at 37°C for 5 minutes, and detached from plate with additional media. Cells were then counted by being resuspended in Trypan blue with a dilution factor of 2 and loaded into a hemocytometer. The

collected cells were centrifuged for 4.5 minutes until a cell pellet was seen and then resuspended with a calculated amount of media in order to gain a cell resuspension of $2.083*10^6$ cells/mL (adding 9.6 ul of cells per 20 ul gel).

SKBR3 breast cancer cells were purchased from ATCC and expanded in McCoy's 5A medium with 10% FBS and 1X Pen/Strep on polystyrene culture plates at 37 °C and 5% CO2 in a humidified environment until 70% confluence, ending culture at passage number 50. Breast cancer cells were passaged and utilized for cell experiments in the same process as for the 3T3 fibroblasts.

MTT Assay

An MTT assay was performed on 3T3 fibroblasts after 1 day in media with peptides adjusted from the protocol provided by the Biotium MTT Cell Viability Assay Kit. Briefly, 3T3 fibroblasts were passaged, resuspended to 20,000 cells/300 ul of DMEM with 10% FBS, and loaded in 300 ul aliquots per well in a 96-well tissue culture plate (3 wells planned for each treatment group). Then, after growing overnight (~18 hours) at 37°C 5% CO2, the DMEM with 10% FBS was aspirated and replaced with 300 ul aliquots of treatment groups containing 6 ul of 50 mM of peptide (totaling 1 mM of peptide), 93.25 ul PBS, and 200.75 ul media: RGD HAVDI, HAVDI only, RGD only, RDG only. A control group of treated cells with only media (no peptide) was utilized as to represent 100% viability. After 1 day in culture at 37°C 5% CO2, conditioned media containing peptides were aspirated, collected, and replaced with 100 ul DMEM without serum (0% FBS) and 100 ul of MTT solution (Biotium) in each well. A control group of DMEM with 0% FBS was added to the plate for a representation of background interference by media and MTT components for end absorbance by plate reading. The 96-well plate with MTT, cells, and media was incubated at 37°C for 4 hours covered in foil as MTT is

photo-sensitive. Then 100 uL DMSO and 100 ul of isopropyl alcohol was added directly to each well in order to solubilize the formazan salt. On Plate Reader Tecan Infinite M200 Pro, the 96-well plate was shaken for 3 minutes at shaking amplitude 1 mm and then the absorbance signal was measured at 570 nm and 630 nm. The background absorbance at 630 nm from the wells containing only DMEM with 0% FBS, MTT, DMSO, and isopropyl alcohol was subtracted from the all signal absorbance values at 570 nm to obtain normalized absorbance values.

Live/Dead Staining

3T3 viability and SKBR3 viability was assessed at 1 day, 3 days, and 5 days using a protocol of a Live/dead stain kit (L3224, Invitrogen) on 20 ul gels with purchased calcein AM (f-actin) and ethidium homodimer-1 (nuclei). Media was changed every other day. Images were taken with fluorescence microscope (Fluorescence Microscope Zeiss Axiophot Vert.A1). Quantification of viability was performed using Image-J software by Otsu thresholding the image and analyzing outlines of particles.

Rhodamine Phalloidin/DAPI Staining

SKBR3-encapsulated in 20 ul gels were fixed after 1 day and 5 days using 4% formaldehyde for 15 min at room temperature. Cytoskeletal staining was performed using rhodamine phalloidin (1 : 40, Biotium) for f-actin with counter staining of 4′,6-diamidino-2-phenylindole (DAPI) (1 : 1000, Biolegend) for nuclei. Images were taken on fluorescence microscope (Fluorescence Microscope Zeiss Axiophot Vert.A1). Ratio of area of f-actin to area of nuclei of spheroids was performed using Image-J software by Minimum thresholding the image and analyzing outlines of particles.

Co-culture set-up

SKBR3 cells were passaged as previously described and then counted in order to obtain a resuspension of 20,000 cells/9.6 ul. Then, 9.6 ul of SKBR3 cell resuspension was added to each well in a 24-well plate. Then 1 mL of DMEM with 1% FBS was added on top of each SKBR3 cell-filled well. Next, 0.3 μm transwell inserts (cleaned with 3 washes of sterile-filtered 70% ethanol and 1 wash of sterile PBS) were added on top of SKBR3-filled wells in order for next cell type to share same media with the SKBR3's. 3T3 cells encapsulated in 20 ul hydrogels (20,000 cells/20 ul gel) were made in syringe tip molds as previously described and set in in 24-well plates. Finally, 300 ul of DMEM with 1% FBS was added on top of the 3T3 gel in order to cover it and the 24-well plate was moved to an incubator at 37°C and 5% CO2. The final look of the set-up for one well is shown in **Figure 4**.

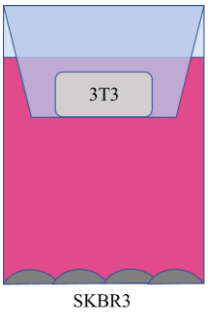

Figure 4. 24-well Co-Culture Set-up

After 5 days in culture, the 3T3 gels were collected, rinsed with PBS 3 times, fixed with 4% formaldehyde for 15 minutes, and then set in PBS to be put into a fridge at 4°C for future staining. The conditioned media was collected into 1.5 mL Eppendorf tubes, spun at 13600 rpm to separate pellet of cell debris, and moved to new Eppendorf tubes to be stored at -80°C. For adhered SKBR3 cells, the wells were washed with PBS and then were filled with 120 ul RLT buffer from a purchased RNeasy Mini Kit. Cells were incubated at room temperature until no

cells were adhered and then the SKBR3 lysate was pooled into sterile Eppendorf tubes (3 gels per Eppendorf tube). RNA extraction was proceeded as instructed by Qiagen.

RNA Extraction

With SKBR3 lysate in RLT buffer, RNA was extracted from SKBR3's per to the Quick-Start Protocol from the RNeasy Mini Kit by Qiagen. Briefly, 1 volume of 70% ethanol was added to the lysate in RLT buffer and mixed by pipetting. 700 ul of sample were moved to RNeasy Mini spin column sitting in a 2 ml tube and centrifuged for 15 seconds at 8000 x g. Then flow-through was discarded. Next, 700 ul of provided RW1 buffer was added to RNeasy spin column and centrifuged for 15 seconds at 8000 x g, discarding flow-through after. Next, 500 ul of provided RPE buffer was added to RNeasy spin column and centrifuged for 15 seconds at 8000 x g, discarding flow-through after, and repeated for 2 minutes. To dry the membrane, the RNeasy spin column was moved to a new 2 ml collection tube and centrifuged at 15000 x g for 1 minute. To elute the RNA, the RNeasy spin column was moved to a new 1.5 ml Eppendorf tube, and 30 ul of RNase free waster was added to the spin column and centrifuged for 1 minute at 8000 x g. RNA purity was tested by measuring absorbance at 260 nm and 280 nm on the NanoDrop Spectrophotometer and calculating the 260/280 ratio. A 260/280 ratio between 1.8 and 2.0 was considered pure RNA. Concentration of RNA at ng/ul was calculated by $c=A*f$ where c is concentration, A is absorbance at 260 nm, and f is $(1/(\varepsilon*b))$ where ε is wavelength dependent absorptivity coefficient and b is pathlength. f utilized for calculations was 40 (ng*cm)/ul for RNA.

cDNA Synthesis

cDNA synthesis from extracted pure RNA of SKBR3's was completed with SuperScript IV Reverse Transcriptase and random 50 μM random hexamers purchased from Invitrogen.

Briefly, 1 ul of 50 μM random hexamers, 1 ul of 10 mM dNTP mix, 11 ul template RNA were mixed briefly in a reaction tube and heated at 65°C for 5 minutes on a thermocycler. Then the RNA-primer mix was incubated on ice for 1 minute. Next, 4 ul of 5x SSIV buffer, 1 ul of 100 mM DTT, 1 ul of RNaseOUT Recombinant RNase Inhibitor, and 1 ul of SuperScript IV Reverse Transcriptase (200 U/ul) were added to the RNA-primer mix and briefly mixed. Then the combined reaction mixture was incubated at 23°C for 10 minutes, incubated at 52.5°C for 10 minutes, and finally incubated at 80°C for 10 minutes. 1 ul of E. coli RNase H was added to combine reaction mixture and incubated at 37°C for 20 minutes. cDNA was stored at -20°C until used for PCR amplification.

Quantitative Polymerase chain reaction (QPCR) Amplification

QPCR was completed with the Brilliant III Ultra-Fast SYBR Green QPCR Master Mix with incorporated reference dye ROX purchased from Agilent and Mx3000P instrument. Briefly, first, the cDNA obtained from cDNA synthesis was diluted with DNase-free water to 5 ng/ul based on the concentration of RNA in order for all cDNA samples to be the same concentration. Then custom primers purchased from Invitrogen (primer sequences in **Appendix**) were reconstituted in DNase-free water to 100 μM and stored at -20°C. When about to be used in PCR, the prepared 100 μM primers were taken out and diluted with DNase-free water to a concentration of 2.5 μM. Lastly, a master mix was prepared by combining 10.3 μl 2x SYBR Green QPCR Master Mix with low Cell ROX, 2 ul of 2.5 μM forward primer, 2 μl of 2.5 μM reverse primer, 2 μl of 5 ng/μl cDNA, and 3.7 μl DNase-free water to reach 20 μl in volume per sample. For every 20 μl sample made, 2 ul of 2.5 μM (2500 nM) primers was used to make the end concentration of primer 250 nM (optimized concentration) and 2 μl of 5 ng/μl cDNA were used to have 10 ng in the sample (optimized amount of cDNA). The total amount of master mix

made was determined by having 3 samples made per peptide group and 3 samples made per primer.

QPCR was run on an AriaMx Real-Time PCR System by Agilent Technologies. The PCR reaction temperatures went in sequence of Hot Start, Amplification, and Melt. Hot Start was one cycle of increasing the temperature to 95°C and holding 95°C for 3 minutes until Amplification. Amplification was 50 cycles of holding 95°C for 5 seconds and then holding 60°C for 10 seconds. Finally, the Melt was one cycle of holding 95°C for 30 seconds, 65°C for 30 seconds, and 95°C for 30 seconds.

GAPDH was housekeeping gene and gave housekeeping cycle threshold (CT). Control group was RGD RDG and gave control CT. The equations to get to expression fold change used are below:

Control ΔCT = Control CT – Housekeeping CT

ΔCT = Sample CT – Housekeeping CT

$\Delta\Delta$CT = Sample ΔCT – Control ΔCT

Expression Fold Change = $2^{-(\Delta\Delta CT)}$

Statistical Analysis

For statistical analysis, a one-way ANOVA with Dunnett's T3 multiple comparisons tests were performed for mechanical characterization and cell studies in a 2D environment ($p < 0.05$). A two-way ANOVA with Sidak's multiple comparisons tests were performed for mechanical characterization and cell studies in a 3D environment and 3D co-culture ($p < 0.05$).

CHAPTER III

RESULTS

Mechanical Characterization

In order to compare the effect of the peptides on the cell behavior in the various gels, we must first show that the only characteristic different among the hydrogels is the peptide type. After making the PEG-peptide hydrogels and swelling them overnight, rheology showed that the hydrogels with combinations of peptides were not significantly different in stiffness and averaged at a storage modulus of 350 Pa, which is stiffer than a normal mouse mammary gland but similar stiffness to a collagen gel used for breast cancer mammosphere formation (**Figure 5A**) (Weigelt, Ghajar and Bissell). Swelling ratios correlated with storage modulus and were only significantly different between RGD HAVDI and RDG RDG, showing that HAVDI peptide caused more swelling (**Figure 5B**). Ultimately, the peptides did not significantly change gel mechanical properties and therefore can be compared for their effect on cells by their bio-instructive roles.

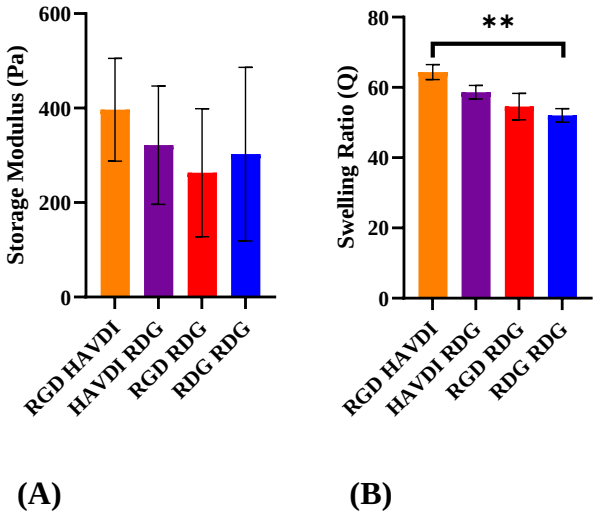

(A) **(B)**

Figure 5. (A) Storage modulus and **(B)** Swelling Ratio of Hydrogels with Different Peptide Combinations (n=3 in both experiments; **p < 0.01)

Cell Studies in 2D Environment

Cytotoxicity of Peptides

Before utilizing the peptides on cells within gels in a 3D environment where the complexities of mechanosensing may change cell behavior, the cytotoxicity of the peptides was tested on 3T3 fibroblasts on cell culture plates in order to ensure the peptides were interacting with the cells but not containing reagents from peptide synthesis that could kill them. After treating 3T3 fibroblasts with the peptides HAVDI, RGD, RDG, and a combination of RGD HAVDI for 1 day in 10% FBS DMEM, an MTT assay shows that the peptides did not significantly decrease cell viability from 100% (**Figure 6A**).

Since in a co-culture, media must be low serum in order for the cells to be signaled by proteins from the the cells, not the serum, 3T3 fibroblasts were also treated with the peptides HAVDI, RGD, RDG, and a combination of RGD HAVDI for 1 day in DMEM with 1% FBS.

Interestingly, an MTT assay showed that the peptides did not significantly decrease 3T3 fibroblast viability from 100% when FBS was lowered from 10% to 1% (**Figure 6B**). Absorbance values at 570 nm indicated that the amount of MTT metabolized was similar in both media groups and was significantly higher in 10% FBS DMEM for 3T3's treated with only HAVDI and only RDG (**Figure 6C**).

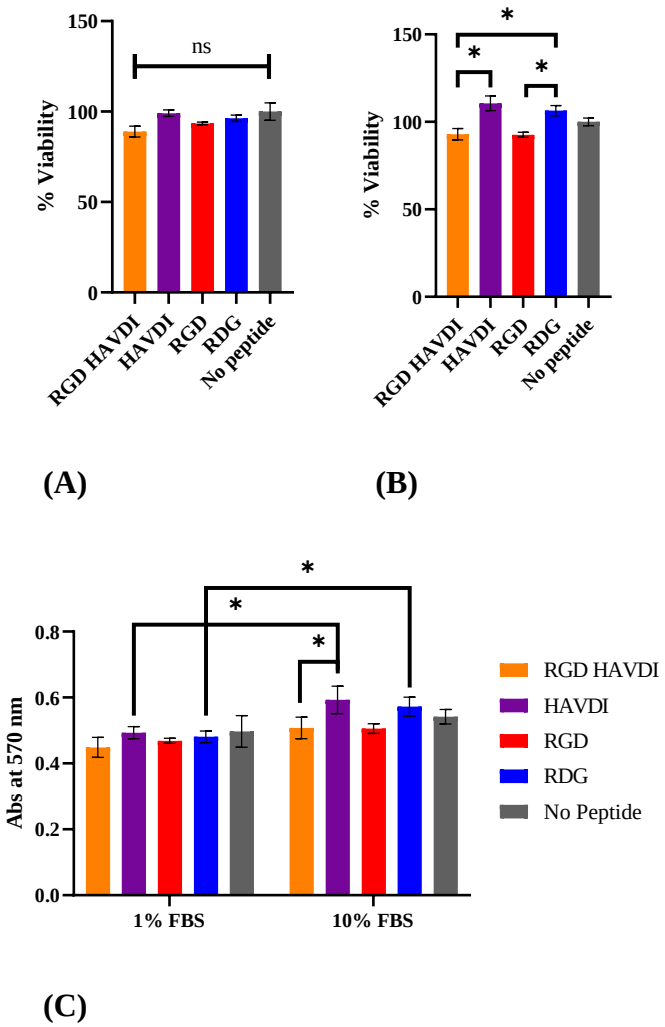

Figure 6. % Viability Of 3T3 Fibroblasts **(A)** adhered to plate treated with 10% FBS DMEM **(B)** adhered to plate treated with 1% FBS DMEM, and **(C)** absorbance values at 570 nm for cells treated with 1% FBS DMEM and 10% FBS DMEM (n=3; *p < 0.5)

Brightfield images taken with DAPI filter of 3T3 fibroblasts adhered to the plate showed 3T3 cells treated with RGD HAVDI and RGD formed clusters, but cells without RGD did not form clusters after 1 day in both media (**Figure 7**).

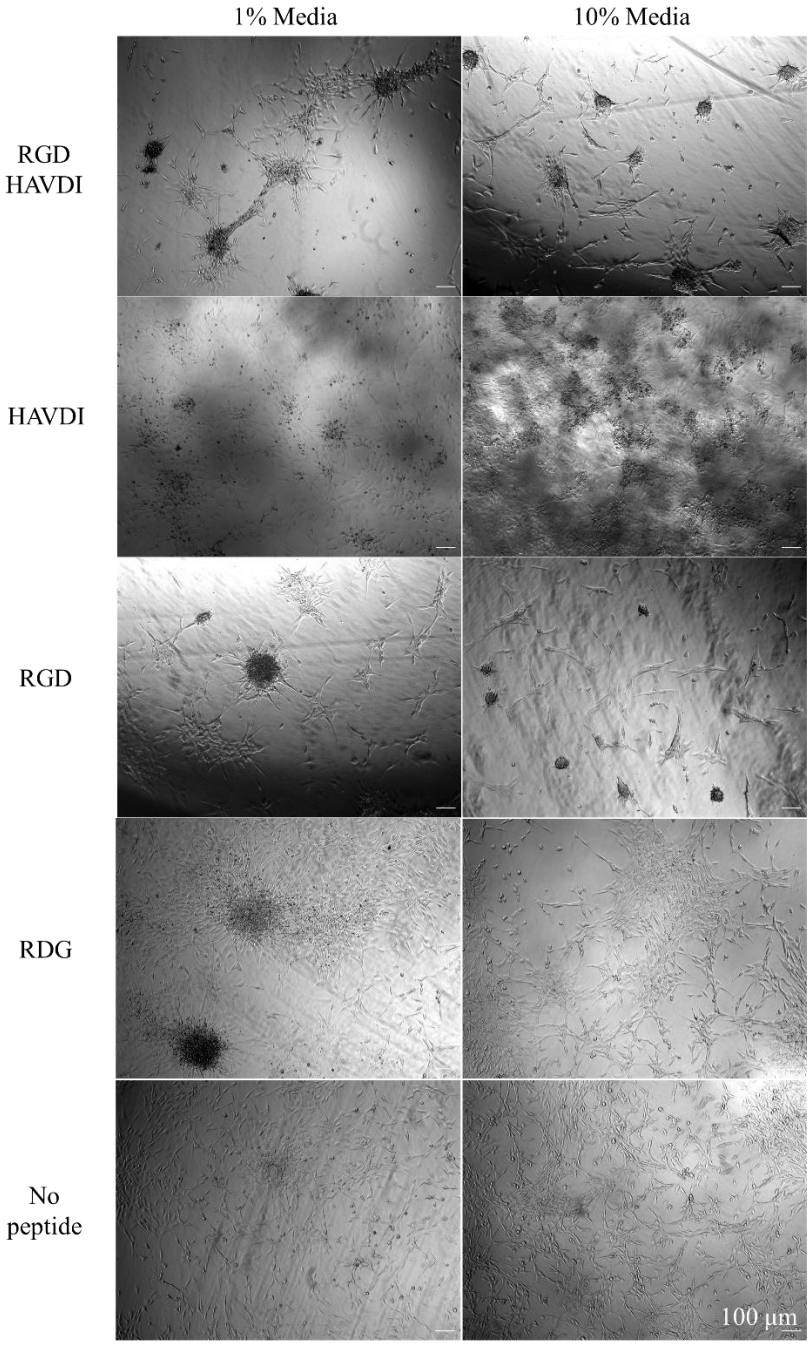

Figure 7. Brightfield Images of 3T3 fibroblasts in 96-well plate (scale bar = 100 μm)

Cell Studies in 3D Environment

Cell Viability

Since cells tend to behave differently in 2D environments and 3D environments since the cells will experience mechanical stimuli on all sides in 3D, fibroblasts and SKBR3's were encapsulated in PEG gels and tested for cell viability. In the hydrogels containing RGD HAVDI, HAVDI RDG, and RGD RDG, 3T3 fibroblasts significantly decreased from 70% to 50% in viability after 3 days (**Figure 8**) from live/dead staining, indicating that the combination of the peptides and the mechanical environment was affecting the fibroblasts viability. The beginnings of spindle-like phenotype normal to fibroblasts was seen in gels with RGD, indicating that RGD peptide was causing the fibroblasts to spread into the gel normally.

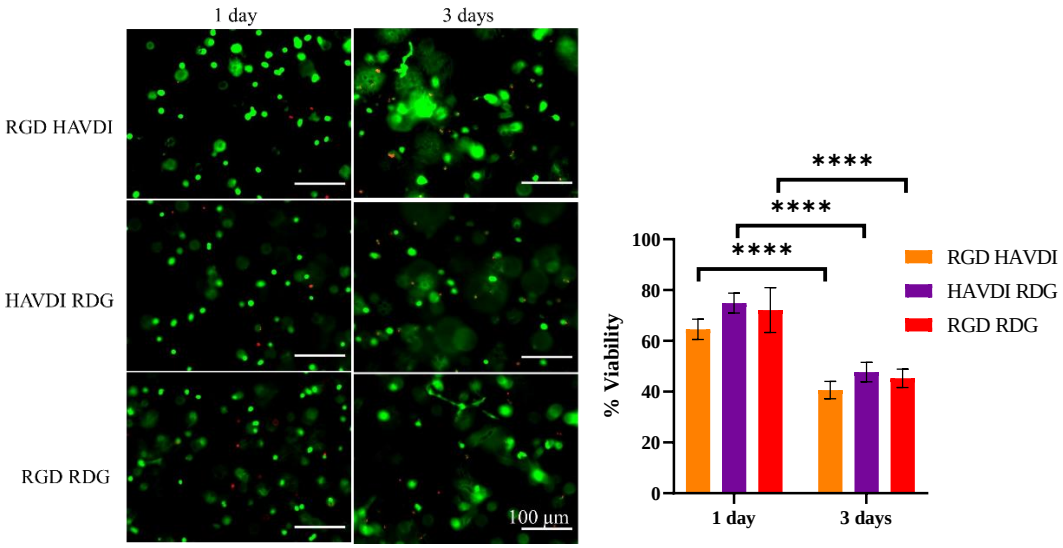

Figure 8. Live/Dead 3T3 fibroblasts in peptide hydrogels 1 day and 3 days (scale bar = 100 µm; n = 3; ****p < 0.0001)

In the hydrogels containing RGD HAVDI, HAVDI RDG, RGD RDG, and RDG RDG, 3T3 fibroblasts maintained a cell viability of 80% after 5 days (**Figure 9**) from live/dead staining. Interestingly, breast cancer cells not able to adhere to the gel seen in the group RDG

RDG did not decrease in viability, indicating that the SKBR3's are experiencing the resistance of anoikis. Resistance to anoikis is known to be a characteristic of cancer where the cancer cells become anchorage-independent and therefore do not commit apoptosis. This is different from normal cells which need anchorage to a substrate to survive or will commit apoptosis (Onder et al.; Guadamillas, Cerezo and Del Pozo).

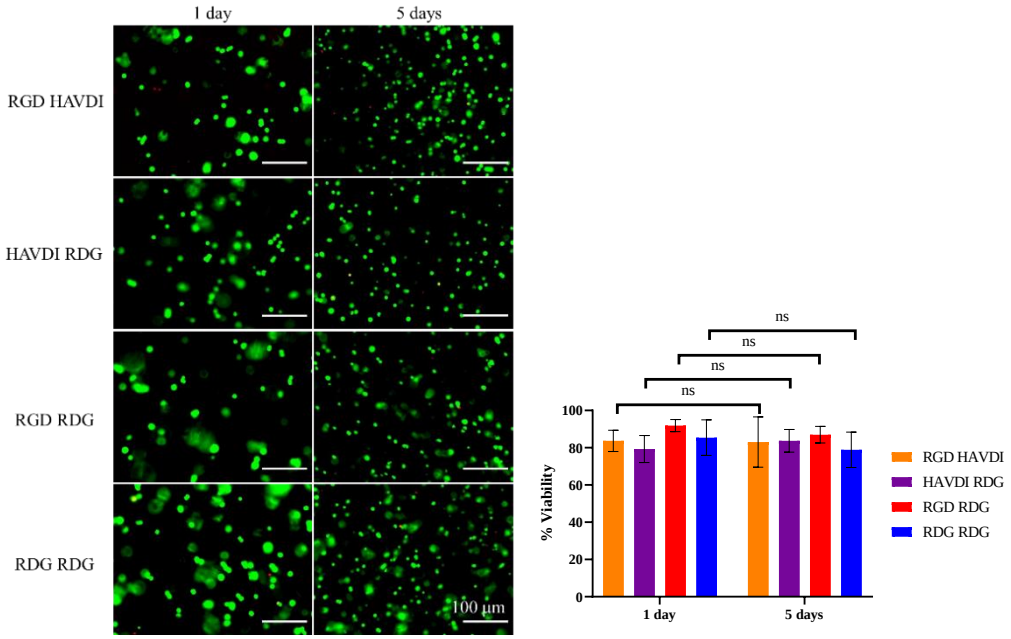

Figure 9. Live/Dead SKBR3 breast cancer cells in peptide hydrogels 1 day and 5 days (scale bar = 100 μm; n = 3)

Also, spheroid formation of SKBR3 cells was seen in all gel formulations despite starting as single cells and the ability for cells to degrade the gel with metalloproteinases (MMPs). Also, the ratio of area of f-actin to area of nuclei was about 1:1 in all gel formulations and were not significantly different between peptide groups (**Figure 10**). Overall, by phenotype alone in a 3D environment, the SKBR3's are showing characteristics of cancer, but not of becoming more mesenchymal-like such as seeing protrusions/spindle-like phenotype.

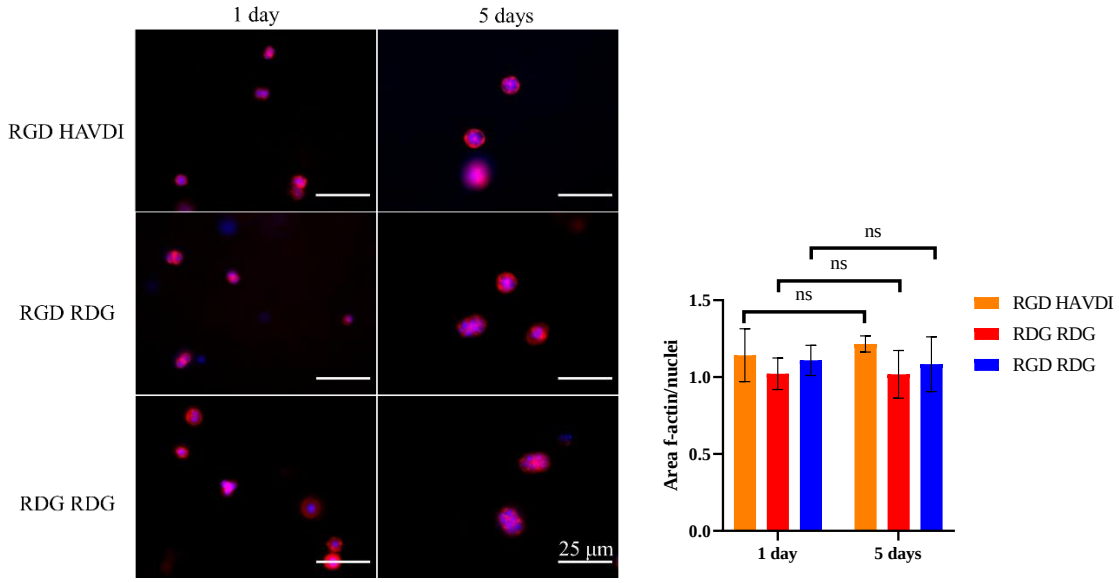

Figure 10. F-actin/nuclei (red/blue) SKBR3 breast cancer cells in peptide hydrogels 1 day and 5 days (scale bar = 25 µm; n = 3)

Cell Studies in 3D Co-Culture

Phenotypic Changes in SKBR3

Since the cell adhesive peptides significantly decreased viability of 3T3's but not SKBR3's in a 3D environment after 3 and 5 days respectively, we were interested in the mRNA expression of the SKBR3's which could correlate with proteins that interact with the 3T3's. Therefore, we set up a co-culture where the 3T3's were encapsulated in hydrogel and set on a transwell insert, while the proteins the 3T3's made were diffused into the media for the SKBR3's on the 24-well plate to interact with. From brightfield images, after 1 day in culture, the SKBR3's with 3T3's interacting with HAVDI peptides gained a spindle-like phenotype while groups without the HAVDI peptide retained their spherical phenotype typical of SKBR3's in normal culture conditions, indicating that the HAVDI peptide was interacting with the 3T3's in a way that caused them to produce proteins that instructed the SKBR3's to become more spindle-

like and more mesenchymal-like (**Figure 11**). Also, the beginnings of spindle-like phenotype in SKBR3's in contact with 3T3 gels with RDG RDG may indicate that the 3T3's inability to adhere to the gel is causing the 3T3's to make proteins that also instruct the SKBR3's to become more spindle-like.

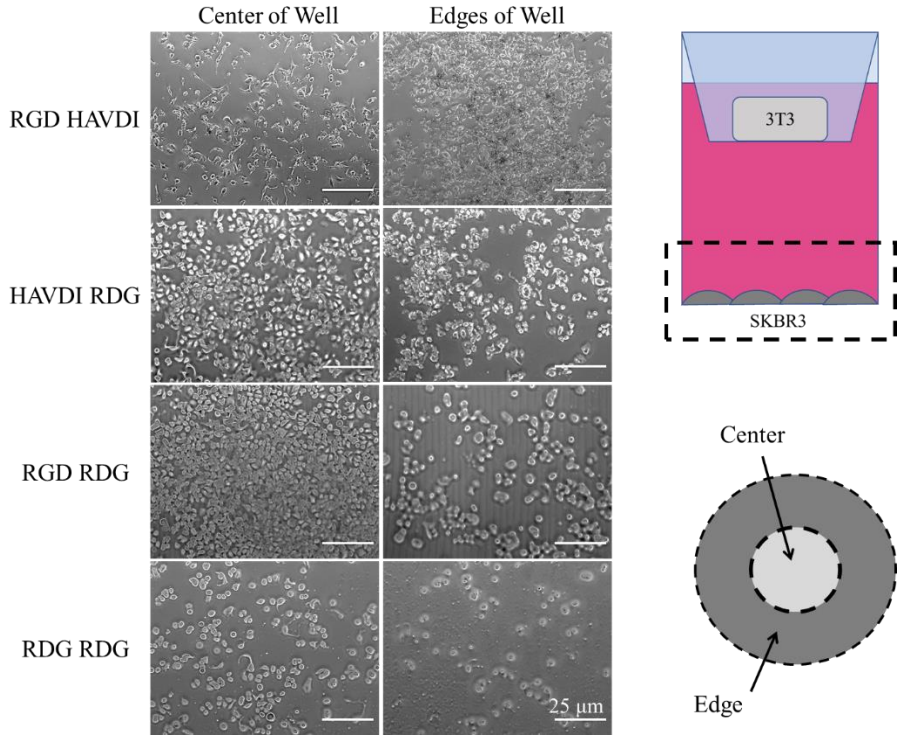

Figure 11. Brightfield images of SKBR3 breast cancer cells on well after 1 day (scale bar = 25 μm)

mRNA Production

We chose four primers for proteins that can be found to upregulated in EMT: fibronectin, vimentin, TGF- β1, and collagen III. After performing QPCR on SKBR3 cells in co-culture with 3T3 gels, the ΔCT values for fibronectin and TGF- β1 were not significantly different among the peptide groups. For vimentin and collagen III, the RGD HAVDI and RDG RDG gels showed the greatest significance in ΔCT values from the control group with no peptide 3T3 gel (**Figure 12**).

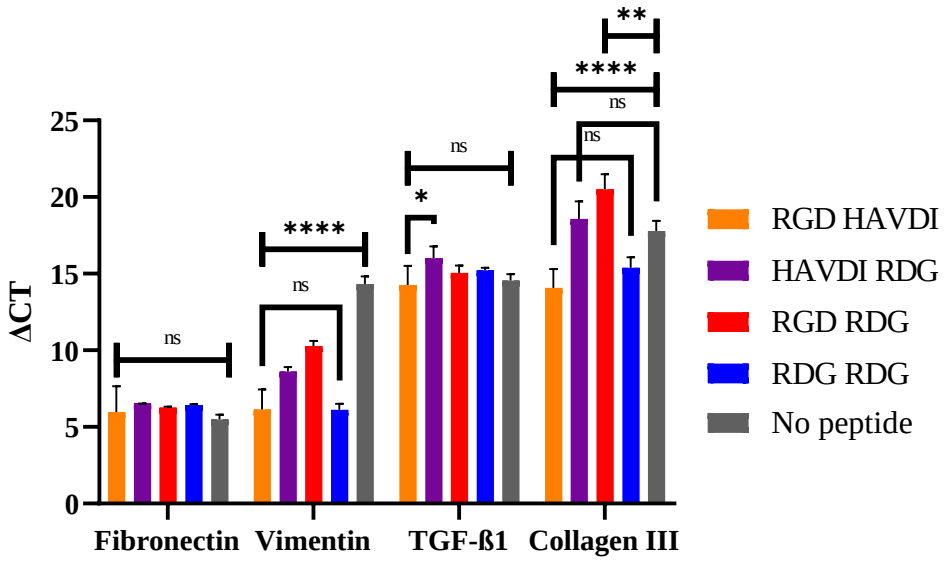

Figure 12. Average ΔCT values (n = 3; *p < 0.05; **p , 0.01; ****p < 0.0001)

ΔCT values were converted to fold change ($2^{-\Delta\Delta CT}$) using RGD RDG as the control group, since cells would normally have access to ECM. SKBR3's expression of mRNA for fibronectin and TGF-β1 was not significantly altered with peptide combinations. However, gels with RGD HAVDI and RDG RDG showed significant increases of mRNA expression for vimentin and collagen III (**Figure 13**).

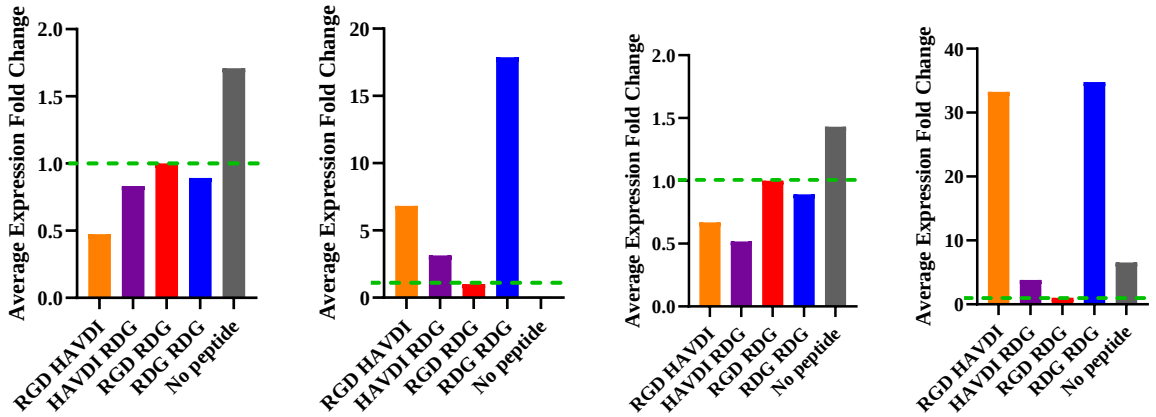

(A) **(B)** **(C)** **(D)**

Figure 13. Expression Fold Change for (**A**) fibronectin, (**B**) vimentin, (**C**) TGF-β1, and (**D**) collagen III where the control group of RGD RDG expression fold change = 1

An increase expression of vimentin and collagen III shows an increase in mesenchymal-like behavior by the breast cancer cells due to the crosstalk between the cancer cells and fibroblasts. Vimentin is an intermediate filament expressed by mesenchymal cells which enables cell motility by interacting with cells' motor proteins and can be considered a marker of fibroblasts (Wu, Grande-Allen and West; Lamouille, Xu and Derynck). Also, vimentin is expressed by epithelial cells, such as SKBR3's, that are undergoing EMT when fibroblasts are initiating EMT in tumor cells (Foster et al.). The interaction of the fibroblasts and the cancer cells explains why the collagen III expression increased in the breast cancer cells. In a wound, fibroblasts deposit ECM such as collagen III which is then replaced by collagen I to facilitate wound contraction along with nerve regeneration and angiogenesis. Similarly in the tumor, fibroblasts generate granulation tissue by deposition of ECM, incite neo-angiogenesis, and

contribute to paracrine signaling with cancer cells (Foster et al.) As the fibroblasts become more cancer-associated, the fibroblasts deposit more collagen in the interstitial matrix leading to desmoplasia, characterized as the buildup of fibrous and connective tissue that forms the firm nodule we call a tumor. Also, human breast cancer cells have been suggested to contribute to the desmoplastic reaction in vivo by producing collagen, suggesting that desmoplasia is formed when the malignant cells are making ECM proteins. The production of vimentin and collagen III by the SKBR3's with a mesenchymal-like phenotype supports that the SKBR3's were experiencing EMT in vitro (Nissen, Karsdal and Willumsen; Zeltz et al.).

Remarkably, the breast cancer cells did not increasingly make TGF- β1 or fibronectin in any of the peptide groups. Both the proteins are typically made when cancer cells are experiencing EMT potentially because a combination of interaction with fibronectin in the interstitial matrix and the reception of active TGF-β is needed to cause the cancer cell to make fibronectin. Since there was a lack of TGF-β in the gel which is usually found in a latent form in natural fibronectin and is activated by proteases, there was no induction of the cancer cells to make more fibronectin. (Lamouille, Xu and Derynck; Park and Schwarzbauer). Also, the increase of vimentin production can be seen without an increase of fibronectin because vimentin has been shown to be able to be synthesized by cells in parallel with collagen III in the EMT HUTECs without the presence of TGF- β1, similar to what the SKBR3's are producing in co-culture with 3T3's in this study (Forino et al.).

Now that the mRNA production from the SKBR3's can be linked to becoming more mesenchymal-like, there still lies the question of why the SKBR3's interacting with 3T3's in the RGD HAVDI gel, representing multiple forms of cellular adhesion sites, show similar mRNA expression with SKBR3's interacting with 3T3's in the RDG RDG gel, representing lack of

cellular adhesion sites. In this study, there is an inclination to treat the HAVDI peptide and RGD peptide as interacting with the cell as individual units when in combination, as if having both peptides present is mimicking cell-cell interactions and cell-ECM interactions at the same time, but the data suggests that that may not be the case. When a cell's integrins grab onto the RGD sequence on ECM, intracellular signaling cascades start with the activation of G-protein Rac1. Active Rac1 then phosphorylates myosin IIA and activates it. Finally, active myosin IIA is recruited to actin in focal adhesions in order to produce contractile stress, contract the cell, and strengthen the cell's interaction with the ECM. When a cell's N-cadherin interacts with the HAV sequence, Rac1 is inhibited (from a mechanism not covered in this paper) and as a result, inhibits the contraction of the myosin-actin complex and recruitment of integrins for focal adhesions even in the presence of RGD. With increased cell-cell interaction, the cell has less ability to mechanically probe its environment, has reduced actin organization, and behaves as if on a softer substrate. Also, since cells generate their own mechanical forces with actin-myosin contractility, loss of the pull of the environment leads to less ECM remodeling and changes in downstream intracellular signaling pathways (Donnelly, Salmeron-Sanchez and Dalby; Cosgrove et al.; Woods et al.; Yano et al.).

With our fibroblasts in a gel with both HAVDI and RGD peptides, it seems that the fibroblasts are losing their interactions with RGD because of the HAVDI's ability to interact with fibroblasts' N-cadherin and then inhibit Rac1 activation, seen with loss of its spindle-like phenotype. Also, since the fibroblasts are anchorage dependent cells and prefer not to attach to each other, the fibroblasts are potentially going through anoikis if not losing the ability to go through apoptosis when cancer-associated (McGill et al.; Ma et al.; Han et al.). Since the HAVDI peptide is not pulling on the fibroblast or connected to another mesenchymal cell when

encapsulated as single cells, the HAVDI peptide is not providing a force needed to keep the fibroblast alive and is inhibiting cell-ECM interaction and the initiation of corresponding intracellular signaling that the RGD provide. Ultimately, both HAVDI RGD and RDG RDG are providing similar environments to the fibroblasts because of the lack of cell-ECM interactions, and the fibroblasts are making proteins that signal to the cancer cells an environment that they can only rely on the cancer cells to recruit them to stay alive.

CHAPTER IV

CONCLUSION

Overall, we found that SKBR3 cells exhibit greater cell viability than 3T3 fibroblasts in the presence of the peptides when encapsulated in PEG gel as single cells, especially without contact with of an ECM peptide. Also, in a co-culture between 3T3's in a gel and SKBR3's on a well, having a synthetic N-cadherin mimetic peptide in the presence of an ECM mimetic peptide or having no ECM mimetic peptide has similar effects on fibroblast behavior as fibroblasts need an ECM mimetic peptide to survive unless they become cancer associated. From the stressed fibroblasts, the breast cancer cells did show that the lack of ECM for the fibroblasts encouraged the cancer cells to become mesenchymal in EMT, seen in a change from spheroidal to spindle-like phenotype and increased expression of mRNA for vimentin and collagen III.

Future analysis of what mRNA and proteins that are being made by the breast cancer cells and fibroblasts in a 2D environment, 3D environment, and 3D co-culture utilizing QPCR and Western blots respectively, would need to be conducted to elucidate what complexities of the cancer cell-fibroblast crosstalk is from the peptides alone, from the opposite cell type, or from the combination of peptide and cell interaction. It would be insightful to evaluate if the SKRB3's display E-cadherins or N-cadherins in response to the peptides as they do not express cadherins in normal culture conditions. Also, evaluating the formation of focal adhesions by 3T3's and SKBR3's by immunostaining would be able to confirm if the HAVDI peptide can inhibit the effects of the RGD peptide.

REFERENCES

Anthis, N. J., and G. M. Clore. "Sequence-Specific Determination of Protein and Peptide Concentrations by Absorbance at 205 Nm." *Protein Sci* 22.6 (2013): 851-8. Print.

Avtanski, D. B., et al. "Honokiol Inhibits Epithelial-Mesenchymal Transition in Breast Cancer Cells by Targeting Signal Transducer and Activator of Transcription 3/Zeb1/E-Cadherin Axis." *Mol Oncol* 8.3 (2014): 565-80. Print.

Avtanski, D., et al. "In Vitro Effects of Resistin on Epithelial to Mesenchymal Transition (Emt) in Mcf-7 and Mda-Mb-231 Breast Cancer Cells - Qrt-Pcr and Westen Blot Analyses Data." *Data Brief* 25 (2019): 104118. Print.

Bellis, S. L. "Advantages of Rgd Peptides for Directing Cell Association with Biomaterials." *Biomaterials* 32.18 (2011): 4205-10. Print.

Bian, L., et al. "Hydrogels That Mimic Developmentally Relevant Matrix and N-Cadherin Interactions Enhance Msc Chondrogenesis." *Proc Natl Acad Sci U S A* 110.25 (2013): 10117-22. Print.

Blaschuk, O. W. "N-Cadherin Antagonists as Oncology Therapeutics." *Philos Trans R Soc Lond B Biol Sci* 370.1661 (2015): 20140039. Print.

Chan, W. C., and P. D. White. *Fmoc Solid Phase Peptide Synthesis: A Practical Approach*. Oxford University Press, 2000. Print.

Chen, C., et al. "Tgfbeta Isoforms and Receptors Mrna Expression in Breast Tumours: Prognostic Value and Clinical Implications." *BMC Cancer* 15 (2015): 1010. Print.

Cosgrove, B. D., et al. "N-Cadherin Adhesive Interactions Modulate Matrix Mechanosensing and Fate Commitment of Mesenchymal Stem Cells." *Nat Mater* 15.12 (2016): 1297-306. Print.

Donnelly, H., M. Salmeron-Sanchez, and M. J. Dalby. "Designing Stem Cell Niches for Differentiation and Self-Renewal." *J R Soc Interface* 15.145 (2018). Print.

Fairbanks, B. D., et al. "Photoinitiated Polymerization of Peg-Diacrylate with Lithium Phenyl-2,4,6-Trimethylbenzoylphosphinate: Polymerization Rate and Cytocompatibility." *Biomaterials* 30.35 (2009): 6702-7. Print.

Fischbach, C., et al. "Cancer Cell Angiogenic Capability Is Regulated by 3d Culture and Integrin Engagement." *Proceedings of the National Academy of Sciences of the United States of America* 106.2 (2009): 399-404. Print.

Forino, M., et al. "Tgfbeta1 Induces Epithelial-Mesenchymal Transition, but Not Myofibroblast Transdifferentiation of Human Kidney Tubular Epithelial Cells in Primary Culture." *Int J Exp Pathol* 87.3 (2006): 197-208. Print.

Foster, D. S., et al. "The Evolving Relationship of Wound Healing and Tumor Stroma." *JCI Insight* 3.18 (2018). Print.

Gu, X., and K. S. Masters. "Regulation of Valvular Interstitial Cell Calcification by Adhesive Peptide Sequences." *J Biomed Mater Res A* 93.4 (2010): 1620-30. Print.

Guadamillas, M. C., A. Cerezo, and M. A. Del Pozo. "Overcoming Anoikis--Pathways to Anchorage-Independent Growth in Cancer." *J Cell Sci* 124.Pt 19 (2011): 3189-97. Print.

Hamley, I. W. "Small Bioactive Peptides for Biomaterials Design and Therapeutics." *Chem Rev* 117.24 (2017): 14015-41. Print.

Han, E. K., et al. "A Cell Cycle and Mutational Analysis of Anchorage-Independent Growth: Cell Adhesion and Tgf-Beta 1 Control G1/S Transit Specifically." *J Cell Biol* 122.2 (1993): 461-71. Print.

Hanahan, D., and R. A. Weinberg. "Hallmarks of Cancer: The Next Generation." *Cell* 144.5 (2011): 646-74. Print.

Harrison, O. J., et al. "The Extracellular Architecture of Adherens Junctions Revealed by Crystal Structures of Type I Cadherins." *Structure* 19.2 (2011): 244-56. Print.

Hazan, Rachel B., et al. "N-Cadherin Promotes Adhesion between Invasive Breast Cancer Cells and the Stroma." *Cell Adhesion and Communication* 4.6 (2009): 399-411. Print.

Holt, Samantha E., et al. "Shooting for the Moon: Using Tissue-Mimetic Hydrogels to Gain New Insight on Cancer Biology and Screen Therapeutics." *MRS Communications* 7.3 (2017): 427-41. Print.

Jivan, F., et al. "Sequential Thiol-Ene and Tetrazine Click Reactions for the Polymerization and Functionalization of Hydrogel Microparticles." *Biomacromolecules* 17.11 (2016): 3516-23. Print.

Koh, B., et al. "Effect of Fibroblast Co-Culture on the Proliferation, Viability and Drug Response of Colon Cancer Cells." *Oncol Lett* 17.2 (2019): 2409-17. Print.

Koistinen, P., and J. Heino. "Integrins in Cancer Cell Invasion." (2000 - 2013). Print.

Lamouille, S., J. Xu, and R. Derynck. "Molecular Mechanisms of Epithelial-Mesenchymal Transition." *Nat Rev Mol Cell Biol* 15.3 (2014): 178-96. Print.

Lim, H. J., et al. "Concentration Dependent Survival and Neural Differentiation of Murine Embryonic Stem Cells Cultured on Polyethylene Glycol Dimethacrylate Hydrogels Possessing a Continuous Concentration Gradient of N-Cadherin Derived Peptide His-Ala-Val-Asp-Lle." *Acta Biomater* 56 (2017): 153-60. Print.

Ma, Z., et al. "Mechanotransduction and Anoikis: Death and the Homeless Cell." *Cell Cycle* 7.16 (2008): 2462-5. Print.

McGill, G., et al. "Loss of Matrix Adhesion Triggers Rapid Transformation-Selective Apoptosis in Fibroblasts." *J Cell Biol* 138.4 (1997): 901-11. Print.

Mrozik, K. M., et al. "N-Cadherin in Cancer Metastasis, Its Emerging Role in Haematological Malignancies and Potential as a Therapeutic Target in Cancer." *BMC Cancer* 18.1 (2018): 939. Print.

Nieberler, M., et al. "Exploring the Role of Rgd-Recognizing Integrins in Cancer." *Cancers (Basel)* 9.9 (2017). Print.

Nieman, M. T., et al. "N-Cadherin Promotes Motility in Human Breast Cancer Cells Regardless of Their E-Cadherin Expression." *J Cell Biol* 147.3 (1999): 631-44. Print.

Nissen, N. I., M. Karsdal, and N. Willumsen. "Collagens and Cancer Associated Fibroblasts in the Reactive Stroma and Its Relation to Cancer Biology." *J Exp Clin Cancer Res* 38.1 (2019): 115. Print.

Onder, T. T., et al. "Loss of E-Cadherin Promotes Metastasis Via Multiple Downstream Transcriptional Pathways." *Cancer Res* 68.10 (2008): 3645-54. Print.

Park, J., and J. E. Schwarzbauer. "Mammary Epithelial Cell Interactions with Fibronectin Stimulate Epithelial-Mesenchymal Transition." *Oncogene* 33.13 (2014): 1649-57. Print.

Patterson, J., and J. A. Hubbell. "Enhanced Proteolytic Degradation of Molecularly Engineered Peg Hydrogels in Response to Mmp-1 and Mmp-2." *Biomaterials* 31.30 (2010): 7836-45. Print.

Perez, T. D., and W. J. Nelson. "Cadherin Adhesion: Mechanisms and Molecular Interactions." *Handb Exp Pharmacol*.165 (2004): 3-21. Print.

Pickup, M. W., J. K. Mouw, and V. M. Weaver. "The Extracellular Matrix Modulates the Hallmarks of Cancer." *EMBO Rep* 15.12 (2014): 1243-53. Print.

Pradhan, S., et al. "Polymeric Biomaterials for in Vitro Cancer Tissue Engineering and Drug Testing Applications." *Tissue Eng Part B Rev* 22.6 (2016): 470-84. Print.

Singh, S. P., et al. "A Peptide Functionalized Poly(Ethylene Glycol) (Peg) Hydrogel for Investigating the Influence of Biochemical and Biophysical Matrix Properties on Tumor Cell Migration." *Biomater Sci* 2.7 (2014): 1024-34. Print.

Wang, F., et al. "The Functions and Applications of Rgd in Tumor Therapy and Tissue Engineering." *Int J Mol Sci* 14.7 (2013): 13447-62. Print.

Wei, L., et al. "Cancer-Associated Fibroblasts Promote Progression and Gemcitabine Resistance Via the Sdf-1/Satb-1 Pathway in Pancreatic Cancer." *Cell Death Dis* 9.11 (2018): 1065. Print.

Weigelt, B., C. M. Ghajar, and M. J. Bissell. "The Need for Complex 3d Culture Models to Unravel Novel Pathways and Identify Accurate Biomarkers in Breast Cancer." *Adv Drug Deliv Rev* 69-70 (2014): 42-51. Print.

Weiss, M. S., et al. "The Impact of Adhesion Peptides within Hydrogels on the Phenotype and Signaling of Normal and Cancerous Mammary Epithelial Cells." *Biomaterials* 33.13 (2012): 3548-59. Print.

Wen, S., et al. "Cancer-Associated Fibroblast (Caf)-Derived Il32 Promotes Breast Cancer Cell Invasion and Metastasis Via Integrin Beta3-P38 Mapk Signalling." *Cancer Lett* 442 (2019): 320-32. Print.

Williams, E., et al. "A Novel Family of Cyclic Peptide Antagonists Suggests That N-Cadherin Specificity Is Determined by Amino Acids That Flank the Hav Motif." *Journal of Biological Chemistry* 275.6 (2000): 4007-12. Print.

Williams, G., E. J. Williams, and P. Doherty. "Dimeric Versions of Two Short N-Cadherin Binding Motifs (Havdi and Inpisg) Function as N-Cadherin Agonists." *J Biol Chem* 277.6 (2002): 4361-7. Print.

Woods, A., et al. "Rac1 Signaling Stimulates N-Cadherin Expression, Mesenchymal Condensation, and Chondrogenesis." *J Biol Chem* 282.32 (2007): 23500-8. Print.

Wu, Y., K. J. Grande-Allen, and J. L. West. "Adhesive Peptide Sequences Regulate Valve Interstitial Cell Adhesion, Phenotype and Extracellular Matrix Deposition." *Cell Mol Bioeng* 9.4 (2016): 479-95. Print.

Yamada, K. M. "Adhesive Recognition Sequences." *J Biol Chem* 266.20 (1991): 12809-12. Print.

Yang, X., et al. "Three-Dimensional-Engineered Matrix to Study Cancer Stem Cells and Tumorsphere Formation: Effect of Matrix Modulus." *Tissue Eng Part A* 19.5-6 (2013): 669-84. Print.

Yano, H., et al. "Roles Played by a Subset of Integrin Signaling Molecules in Cadherin-Based Cell-Cell Adhesion." *J Cell Biol* 166.2 (2004): 283-95. Print.

Zeitouni, S., et al. "Human Mesenchymal Stem Cell-Derived Matrices for Enhanced Osteoregeneration." *Sci Transl Med* 4.132 (2012): 132ra55. Print.

Zeltz, C., et al. "Cancer-Associated Fibroblasts in Desmoplastic Tumors: Emerging Role of Integrins." *Semin Cancer Biol* 62 (2020): 166-81. Print.

APPENDIX

Peptide schematics

KCGPQGIQGQCK (KCGPQ-W) peptide

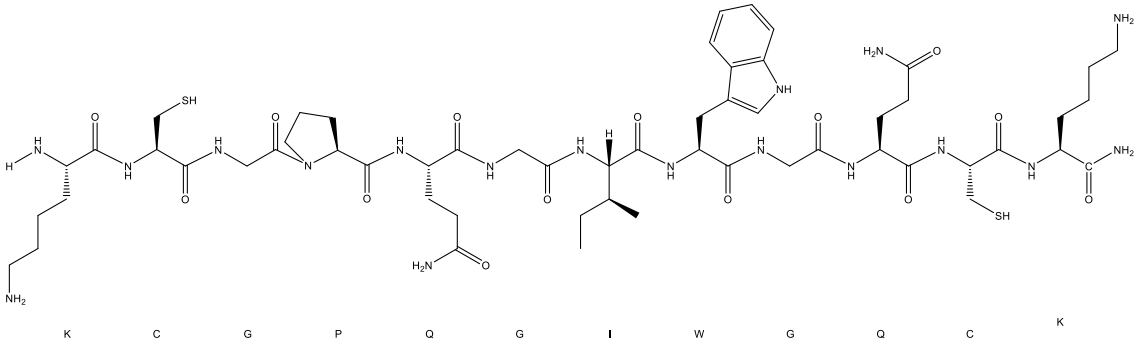

CGRGDS (RGD) peptide

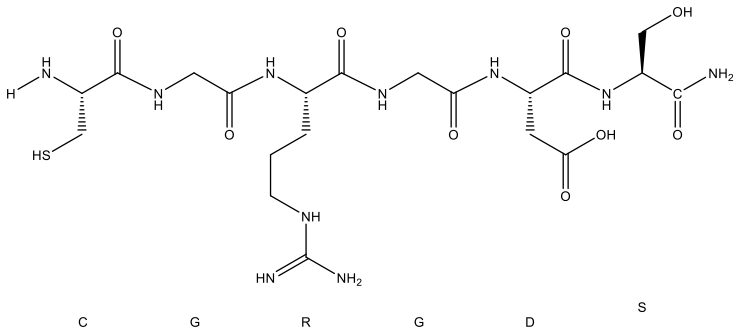

CGRDGS (RDG) peptide

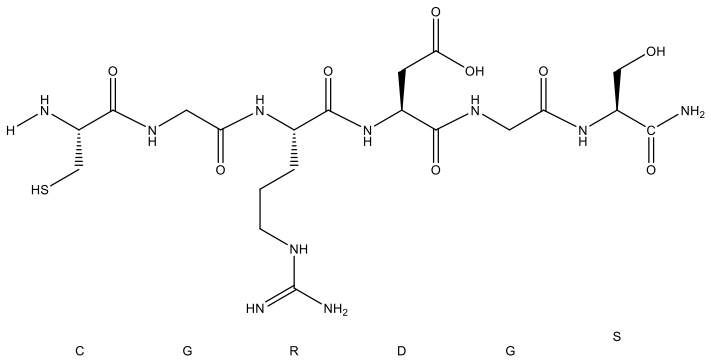

HAVDIGGGC (HAVDI) peptide

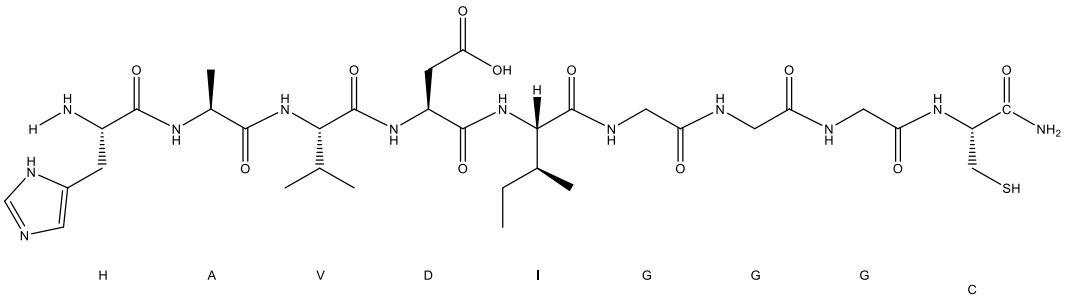

8-arm, 40K PEG-NB

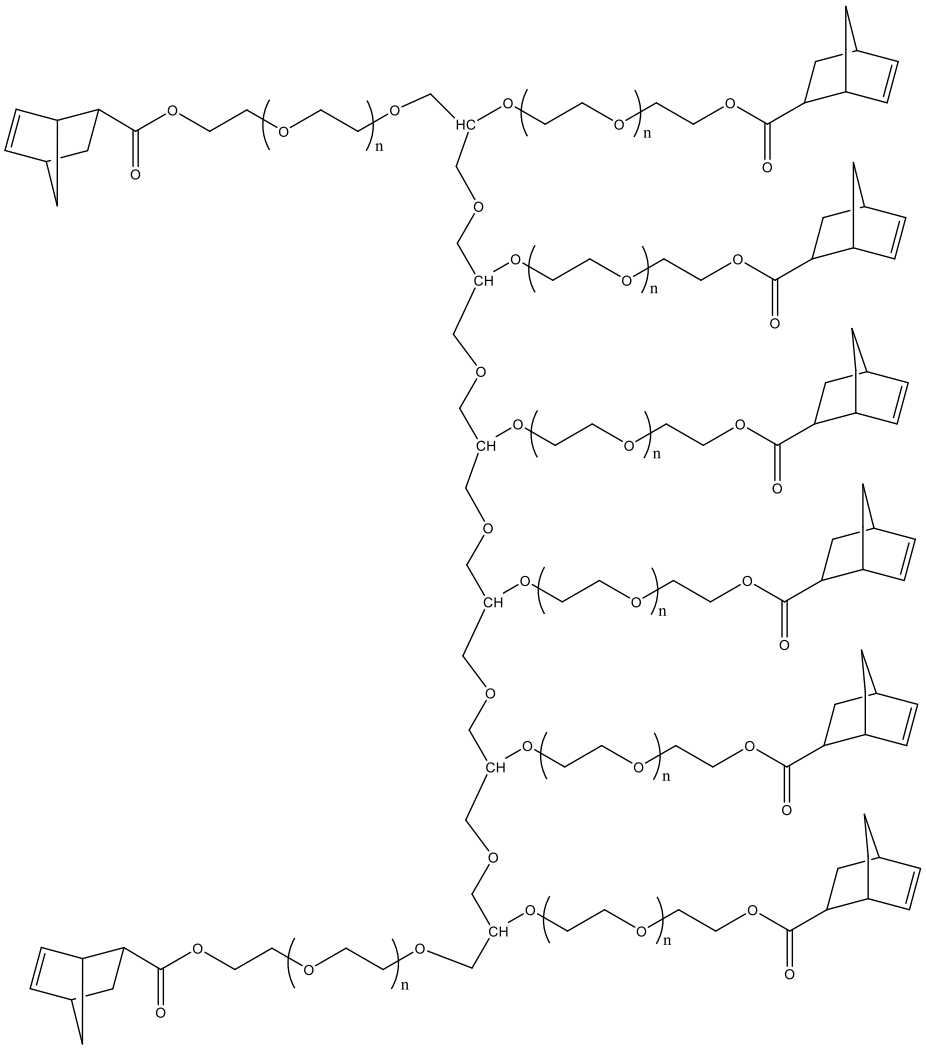

MALDI+

KCGPQ-W

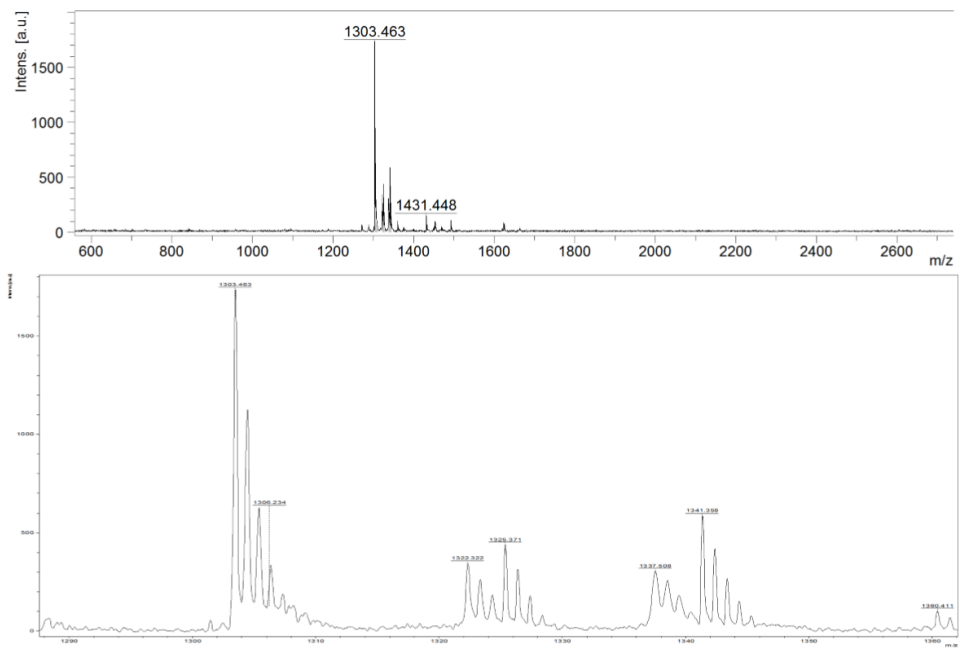

Target
Position A6

Laser
Laser beam attenuation 45.741
Laser repetition rate 60 Hz
Number of shots 154

Spectrometer
positive voltage polarity POS
PIE delay 110 ns
Ion source voltage 1 19 kV
Ion source voltage 2 15.65 kV
Lens voltage 9.8 kV
Linear detector voltage 2.784 kV
Deflection on
Deflection mass
SampleRate 0.5 ns

Reflector voltage 1 20 kV
Reflector detector voltage 1.845 kV

MSMS parent mass

Instrument
Instrument type microflex
Serial instrument number 256969.00080
Name of computer LIU-41-Z440-1
Operator ID or name BDAL@DE
flexControl version flexControl 3.4.135.0
flexAnalysis version

RGD

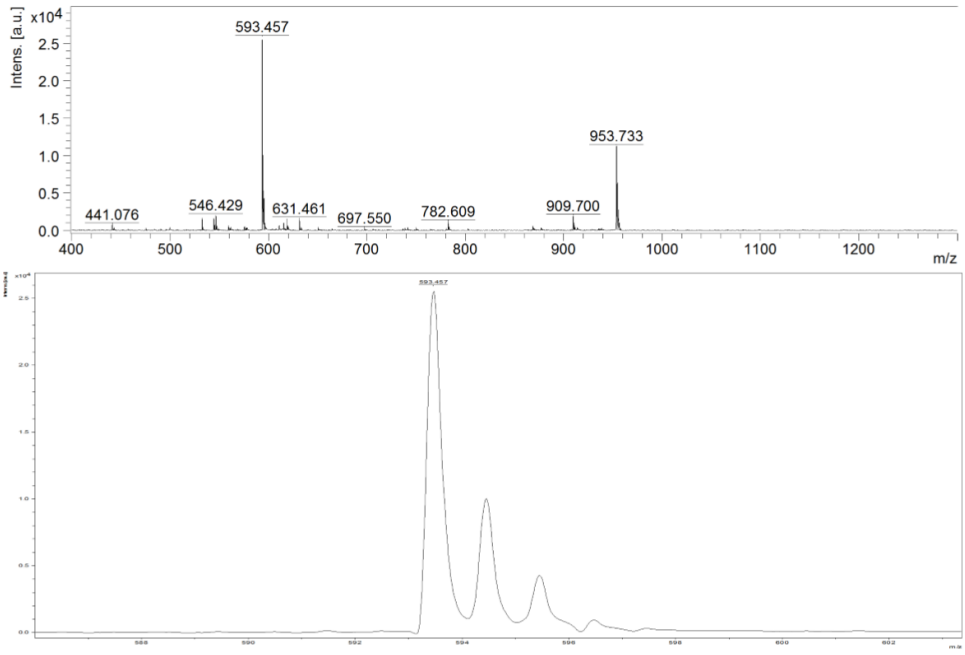

Target
Position D8

Laser
Laser beam attenuation 26.296
Laser repetition rate 60 Hz
Number of shots 311

Spectrometer
positive voltage polarity POS
PIE delay 110 ns
Ion source voltage 1 19 kV
Ion source voltage 2 15.65 kV
Lens voltage 9.8 kV
Linear detector voltage 0 kV
Deflection on
Deflection mass
SampleRate 0.5 ns

Reflector voltage 1 20 kV
Reflector detector voltage 1.944 kV

MSMS parent mass

Instrument
Instrument type microflex
Serial instrument number 256969.00080
Name of computer LIU-41-Z440-1
Operator ID or name BDAL@DE
flexControl version flexControl 3.4.135.0
flexAnalysis version

ESI+

HAVDI

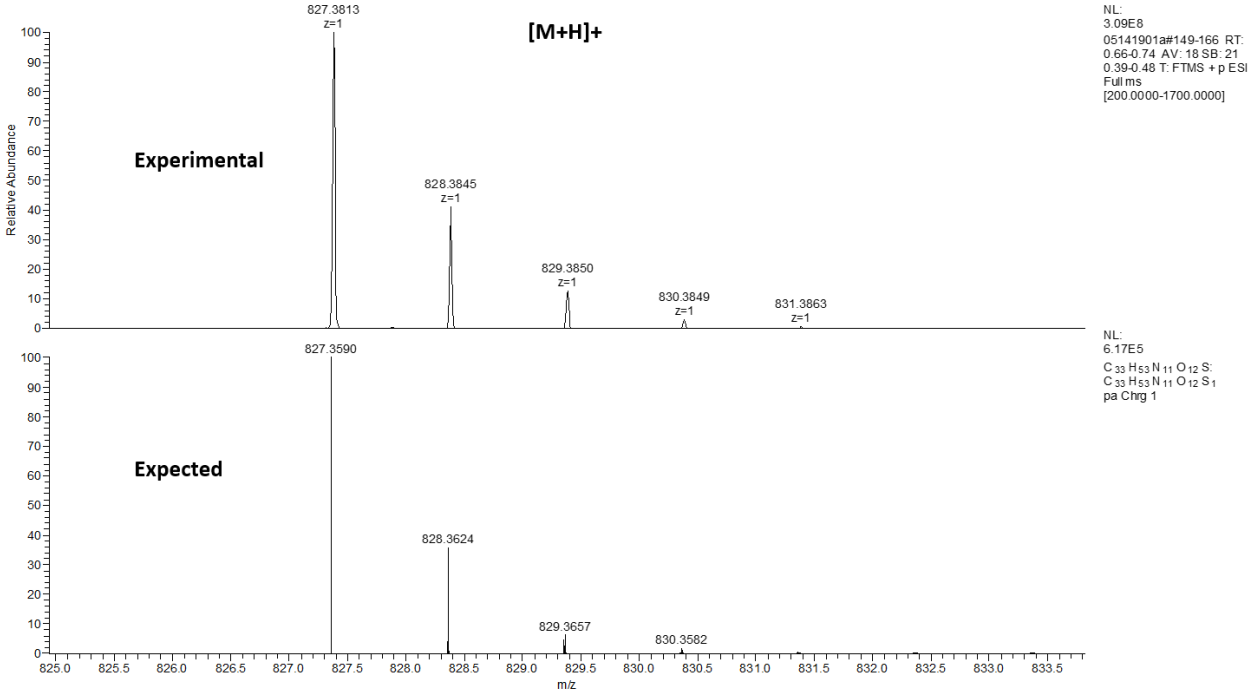

RDG

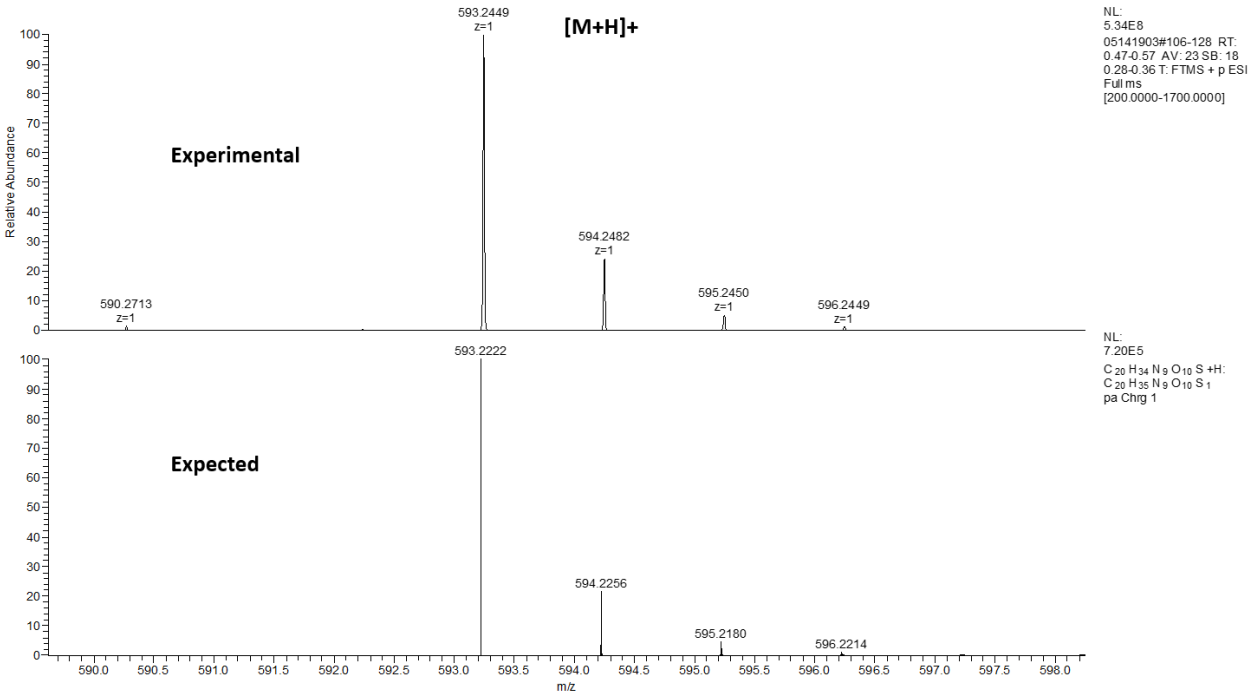

RT-PCR Primer Sequences

Gene	Species	Forward (5'-3')	Reverse (5'-3')	Melting Temp (°C)	Reference
Fibronectin	Human	ATGATGAGGTGCACGTGTGT	CTCTGAATCCTGGCATTGGT	58	(D. Avtanski et al.) (D. B. Avtanski et al.)
Vimentin	Human	AGATGGCCCTTGACATTGAG	TGGAAGAGGCAGAGAAATCC	58	(D. Avtanski et al.) (D. B. Avtanski et al.)
GAPDH	Human	CTCTCTGCTCCTCCTGTTCGAC	TGAGCGATGTGGCTCGGCT	60	(Zeitouni et al.)
TGF-β1	Human	TCGCCAGAGTGGTTATCTT	TAGTGAACCCGTTGATGTCC	55	(Chen et al.)
Collagen III	Human	GGGAACAACTTGATGGTGCTACT	TCAGACATGAGAGTGTTTGTGCAA	60	(Zeitouni et al.)